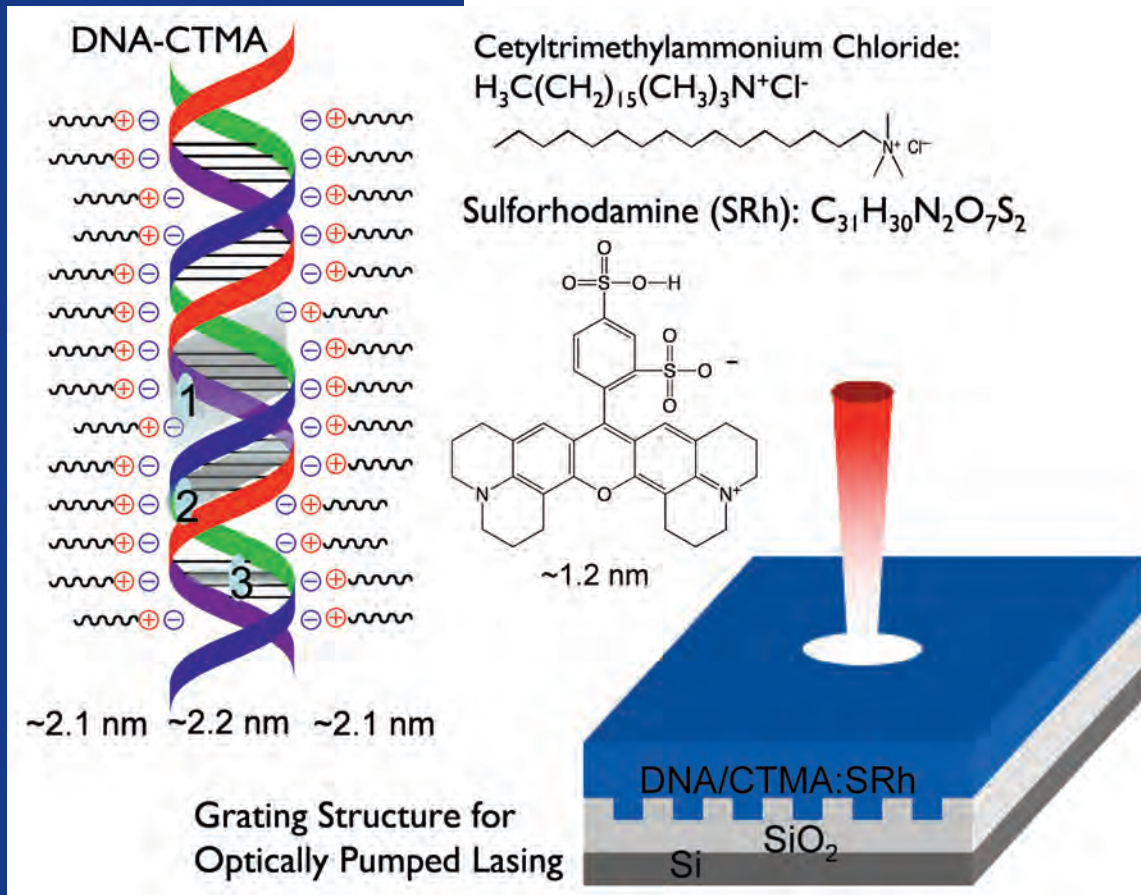


# Applied Optics



# Photoluminescence and lasing from deoxyribonucleic acid (DNA) thin films doped with sulforhodamine

Z. Yu, W. Li, J. A. Hagen, Y. Zhou, D. Klotzkin, J. G. Grote, and A. J. Steckl

Thin solid films of salmon deoxyribonucleic acid (DNA) have been fabricated by treatment with a surfactant and used as host for the laser dye sulforhodamine (SRh). The DNA films have an absorption peak at  $\sim 260$  nm owing to absorption by the nitrogenous aromatic bases. The SRh molecules in the DNA films have absorption and emission peaks at 578 and 602 nm, respectively. The maximum emission was obtained at  $\sim 1$  wt. % SRh in DNA, equivalent to  $\sim 100$  DNA base pairs per SRh molecule. A distributed feedback grating structure was fabricated on a  $\text{SiO}_2$ -Si substrate using interference lithography. The grating period of 437 nm was selected, corresponding to second-order emission at the amplified spontaneous emission wavelength of 650 nm. Lasing was obtained by pumping with a doubled Nd:YAG laser at 532 nm. The lasing threshold was  $3 \mu\text{J}$ , corresponding to  $\sim 30 \mu\text{J}/\text{cm}^2$  or  $4 \text{ kW}/\text{cm}^2$ . The emission linewidth decreased from  $\sim 30$  nm in the amplified spontaneous emission mode to  $< 0.4$  nm (instrument limited) in the lasing mode. The slope efficiency of the lasing was  $\sim 1.2\%$ . © 2007 Optical Society of America

OCIS codes: 050.2770, 140.2050, 140.3580, 160.2540, 160.5470.

## 1. Introduction

Biological materials represent a rich and mainly untapped resource for photonic and electronic devices. Biomaterials have many attractive features: unusual optical and electrical properties that are not readily reproduced in manmade materials, they are a widely available and replenishable resource, and they are biodegradable and environmentally friendly. The integration of biological materials with semiconductors is a particularly fertile area with many applications.<sup>1</sup> Because of its primacy in biological reproduction, deoxyribonucleic acid (DNA) has been a subject of investigation by molecular biologists and other life scientists for several decades. More recently, the unique nanostructure and replication properties of DNA molecules have started to be investigated by physical scientists and engineers interested in incorporating these properties in new or improved devices.<sup>2</sup> Studies<sup>3,4</sup> of the electro-optical properties of DNA-based materials

have opened doors to novel device implementation. For example, organic light emitting diodes (OLED) containing DNA electron blocking layers have been recently reported<sup>5</sup> to exhibit significant enhancements in luminance and luminous efficiency compared to conventional OLED without the DNA layer.

Organic solid-state lasers using a variety of host and lumophore combinations have made steady progress<sup>6-11</sup> in the last decade in terms of wavelength tunability, reduced threshold, and increased. Polymeric matrices have been found<sup>12</sup> to be an extremely important factor in influencing lasing properties such as intensity, threshold, and optical gain. DNA is reported<sup>13</sup> to be an efficient host for certain luminescent organic and organometallic molecules in both solution and solid-state thin films. In this paper we report on the use of DNA as a host material for optically pumped organic solid-state lasers.

## 2. Experimental Methods

The starting DNA material used in this study is derived from salmon sperm<sup>14</sup> and was provided by the Chitose Institute of Science and Technology (CIST) in Japan. After purification and protein removal, the freeze-dried DNA remains water soluble, which impairs the possibility for thin-film formation and incorporation into device structures. To change the solubility, a cationic surfactant reaction was used<sup>15</sup> to convert DNA to a DNA-lipid complex. Cetyltrimethylammonium chloride (CTMA) was used to form a

Z. Yu, W. Li, J. A. Hagen, Y. Zhou, D. Klotzkin, and A. J. Steckl (a.steckl@uc.edu) are with the Nanoelectronics Laboratory, University of Cincinnati, Cincinnati, Ohio 45221-0030. J. G. Grote is with the U.S. Air Force Research Laboratory, Wright-Patterson Air Force Base, Ohio 45324.

Received 4 August 2006; revised 21 November 2006; accepted 24 November 2006; posted 28 November 2006 (Doc. ID 73775); published 1 March 2007.

0003-6935/07/091507-07\$15.00/0

© 2007 Optical Society of America

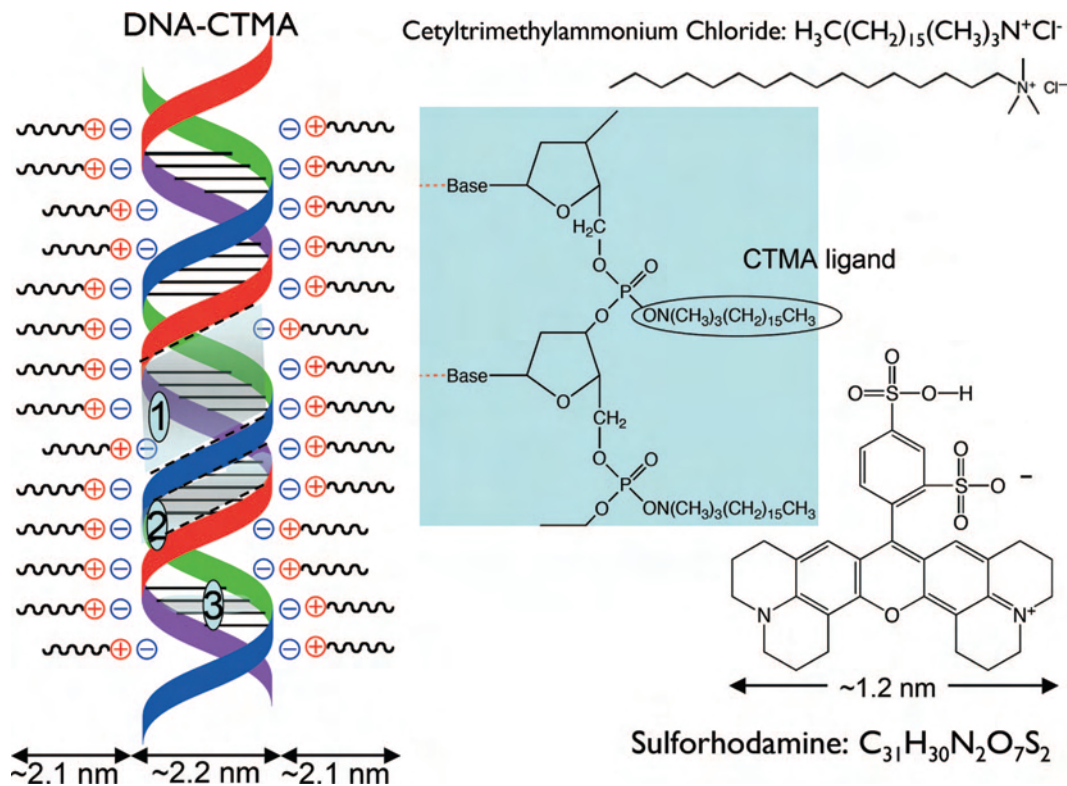


Fig. 1. (Color online) DNA and sulforhodamine structures with possible site for intercalation.

DNA-CTMA complex as shown in Fig. 1, which is not soluble in water but can be dissolved in organic solvents (alcohols). The as-received DNA has a molecular weight (MW) of the order of several million daltons. A sonication process<sup>16</sup> was utilized to reduce the DNA MW to 150–200 kDa. For comparison to DNA, we have also used poly(methyl methacrylate) (PMMA) with a MW of 120 kDa (Sigma-Aldrich) as a lumophore host material. PMMA is known<sup>17,18</sup> as a solid-state dye laser host.

The laser dye sulforhodamine 640 (SRh) (Exciton Inc. Dayton, Ohio) was used as the lumophore. SRh, which is a member of the popular rhodamine family of dyes, has maximum absorption and fluorescence emission at 578 and 602 nm, respectively. When used in dye laser applications in solution, its lasing wavelength ranges from 610 to 670 nm depending on solvent type and pumping source. The structure of the SRh molecule is shown in Fig. 1.

To vary SRh doping concentration in DNA-CTMA and PMMA thin films, solid DNA-CTMA and SRh powder were mixed and dissolved in butanol solution with different weight ratios. PMMA granules and SRh powder were mixed and dissolved in cyclopentanone and methanol mixture. Both DNA-CTMA and PMMA were controlled at 5 wt. % in their respective solutions. The solutions were stirred for 12 h at room temperature to completely dissolve the dye and host materials and to improve the uniformity of mixing. For the photoluminescence (PL) measurements, fused silica wafers from General Electric were used as substrates. Thin films were spin coated on the

wafers at 500 rpm for 10 s ramping up to 3000 rpm for 30 s for DNA-CTMA films and 500 rpm for 10 s ramping up to 4000 rpm for 30 s for PMMA films. These conditions produced DNA-CTMA films of ~80 nm and PMMA films of ~140 nm. The films were baked in a vacuum oven at 30 mbars and 80 °C for 60 min to remove any extra solvent.

Various approaches have been utilized<sup>6</sup> for the design of organic laser cavity structures, including multilayer microcavity, waveguide distributed feedback (DFB), and distributed Bragg reflection (DBR). We have used the DFB grating structure shown in Fig. 2 to provide feedback by Bragg scattering.<sup>19</sup> A DFB template structure was patterned on oxidized ( $\text{SiO}_2 \sim 3 \mu\text{m}$ ) Si  $\langle 100 \rangle$  wafers. At the wavelength of SRh lasing (650 nm) we have measured the following refractive indices:  $n \approx 1.46$  for the  $\text{SiO}_2$  layer on Si,  $n \approx 1.5$  for the DNA layer, and  $n \approx 1.49$  for the PMMA. Therefore light confinement in the DNA-CTMA or PMMA layers is provided by the  $\text{SiO}_2$  layer underneath and with air serving as the upper confinement layer. An Si  $\langle 100 \rangle$  substrate was chosen for easy cleaving. The period of the DFB was determined according to the well-known Bragg equation

$$2\Lambda = p \frac{\lambda_B}{n_{\text{eff}}},$$

where  $\Lambda$  is the period of grating,  $\lambda_B$  is the Bragg wavelength of (emitted) light,  $n_{\text{eff}}$  is the effective index of refraction, and  $p$  is the grating order (1, 2, 3, ...).

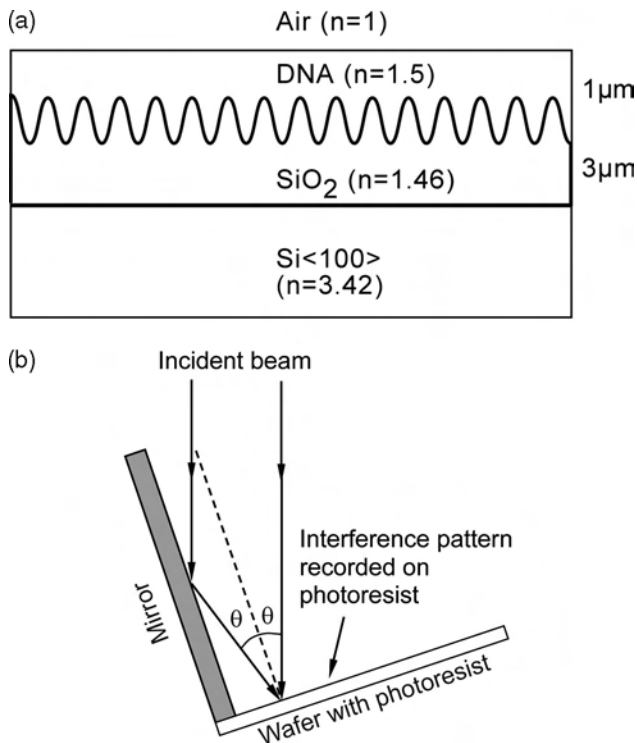


Fig. 2. DFB laser grating. (a) Structure, (b) Lloyd mirror interference lithography.

The period was selected for second-order operation ( $p = 2$ ) to provide surface emission, which is more easily measured, while providing feedback at wavelengths within the gain region of the dye. We used a nominal grating period of 437 nm for the structure to enable SRh laser emission at approximately 650 nm.

The DFB pattern was fabricated using Lloyd's mirror interference lithography (IL), which generates an optical interference pattern between a directly incident component and a reflected component originating from the same laser beam as shown schematically in Fig. 2. The IL system uses a He–Cd laser at 325 nm as the light source. The relationship between the interference pattern period  $\Lambda$  and the incident angle  $\theta$  is given by

$$\Lambda = \frac{\lambda_{\text{He-Cd}}}{2 \sin \theta},$$

where  $\lambda_{\text{He-Cd}}$  is the wavelength of the He–Cd laser, and  $\theta$  is half the angle between directly incident and reflected components. The IL pattern is imprinted in a photoresist layer (Shipley 1805) on the  $\text{SiO}_2$ –Si wafer. A thin (100 nm) Al layer is placed between the photoresist and the  $\text{SiO}_2$  layer to provide a robust thin-film mask for subsequent etching. The Al is patterned by wet etching in a phosphoric–nitric–acetic acid mixture. Next, the grating pattern is transferred into the  $\text{SiO}_2$  layer to form the DFB template by plasma etching in  $\text{NF}_3/\text{Ar}$  (10/5 sccm, standard cubic centimeters per minute) using a Plasma-Therm 790 system in the inductively coupled plasma (ICP) mode.

The etching conditions were 500 W ICP power, 100 W rf power, and a pressure of 5 mTorr. We used a 2 min etch time to produce a uniform periodic structure with a grating depth of  $\sim 200$  nm.

The active organic layer (1  $\mu\text{m}$  thick) doped with SRh (1 wt. %) is spin coated on top of the DFB template and baked at 95  $^\circ\text{C}$  for 30 min. For amplified spontaneous emission (ASE) measurements,  $\text{SiO}_2$ –Si wafers without the DFB grating were used as substrates.

A Perkin-Elmer spectrometer was used to measure the optical absorption of the various thin films deposited on quartz substrates. The PL measurements were performed with a He–Cd laser photoexcitation at 325 nm. The emission spectra were analyzed by an Acton Research spectrometer equipped with a photomultiplier sensitive in the UV-visible spectrum. High-pass filters and dichroic mirrors were utilized to block the laser pump light. The spectrometer resolution was 0.16 nm, and all PL measurements were performed at 300 K.

The excitation source for the ASE and lasing was a frequency-doubled Nd:YAG laser (Spectra-Physics, Mountain View, California) operated at 532 nm, 8 ns pulse duration with a repetition rate of 10 Hz. The beam diameter on the sample was 3.5 mm. A neutral density filter wheel was used to adjust the pump energy. An Ocean Optics (Dunedin, Florida) fiber-coupled CCD spectrometer with 0.1 nm resolution was used to record the spectra, and Newport (Irvine, California) power and energy detectors were used to measure the emitted output.

### 3. Results and Discussion

#### A. Photoluminescence

The basic optical properties of thin films of the hosts and dye molecules were characterized first: absorption (for DNA, PMMA, and SRh) and PL (for undoped

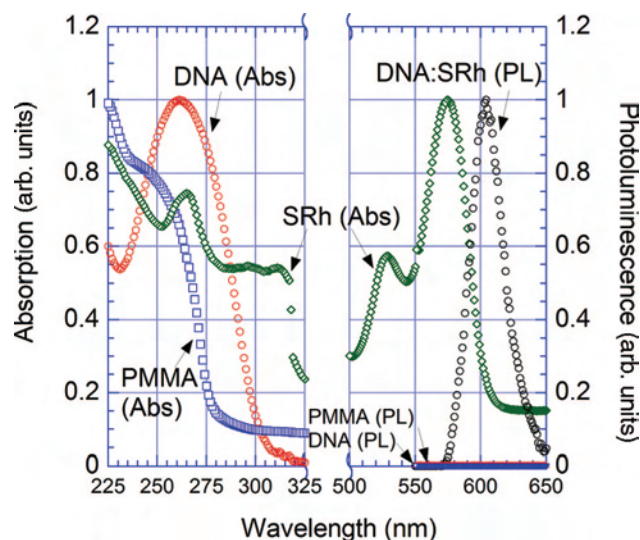


Fig. 3. (Color online) Absorption spectra of undoped DNA and PMMA and sulforhodamine 640 (SRh) thin films and PL spectra for undoped DNA and PMMA and DNA:SRh.

DNA and PMMA, and DNA:SRh). A representative set of absorption and PL spectra is shown in Fig. 3. The DNA film exhibits its well-known UV absorption peak at 260 nm owing to the presence of aromatic nitrogenous bases. The PMMA film also shows an absorption edge in the UV. The SRh film has its major absorption peak at 578 nm. The DNA:SRh film has strong emission from the SRh molecules at 605 nm, consistent with values reported in the literature. The small Stokes shift between the SRh emission and absorption ( $\Delta\lambda \approx 30$  nm) can lead to residual self-absorption. The DNA:SRh PL peak has a width of  $\sim 35$  nm. The undoped DNA and PMMA films showed no visible PL emission, including in the orange-red region of the SRh emission.

To determine the optimal doping concentration for PL emission, DNA and PMMA thin films containing a range of SRh concentrations were photoexcited under the same PL conditions. All samples showed peak emission at 605 nm. The integrated PL intensities for DNA:SRh and PMMA:SRh (multiplied 5 $\times$ ) at approximately the peak emission at 605 nm are plotted as a function of SRh weight percent in Fig. 4(a). The maximum PL emission is achieved for an SRh concentration of 0.75–1 wt. % in both the DNA and the PMMA films. Clearly the DNA is a much more efficient host material (by a factor of  $\sim 17\times$ ) than PMMA, without even taking into consideration that the PMMA films were nearly twice the thickness of the DNA films. The insets in Fig. 4(a) show photographs of the PL emission of DNA and PMMA films doped with 0.7 wt. % SRh.

To take into consideration the molecular structure difference between DNA and PMMA, Fig. 4(b) plots the PL intensity versus the DNA base pairs and the MMA monomer numbers (in PMMA) per SRh molecule. The maximum PL intensity in the DNA:SRh films occurs at a ratio of base pairs to SRh molecules of 100:1. The corresponding maximum in the PMMA:SRh films takes place at a MMA:SRh ratio of 1000:1.

It is interesting to consider the reasons for the ability of the DNA films to emit light more efficiently than other polymers. The intercalation of certain lumophores between DNA base pairs, which is frequently reported as a very sensitive signature of the presence of DNA molecules,<sup>20</sup> could be the reason for the efficient luminescence. Lumophore molecules may be more effectively prevented from exchanging energy when shielded by the base pairs in the DNA structure. Furthermore, the tight spatial fit between lumophore molecules and the base pair structure may minimize (or prevent) the conformational relaxation of excited lumophores and thereby enhance the process of radiative relaxation.

The circular dichroism (CD) property, namely the difference in optical absorption of clockwise and counterclockwise circularly polarized light, identifies the presence of chiral materials. DNA because of its double helix structure has a well-known<sup>21</sup> CD spectrum. CD spectroscopy was used to investigate the structural relationship between the DNA and the SRh molecules. One practical limitation of the interpreta-

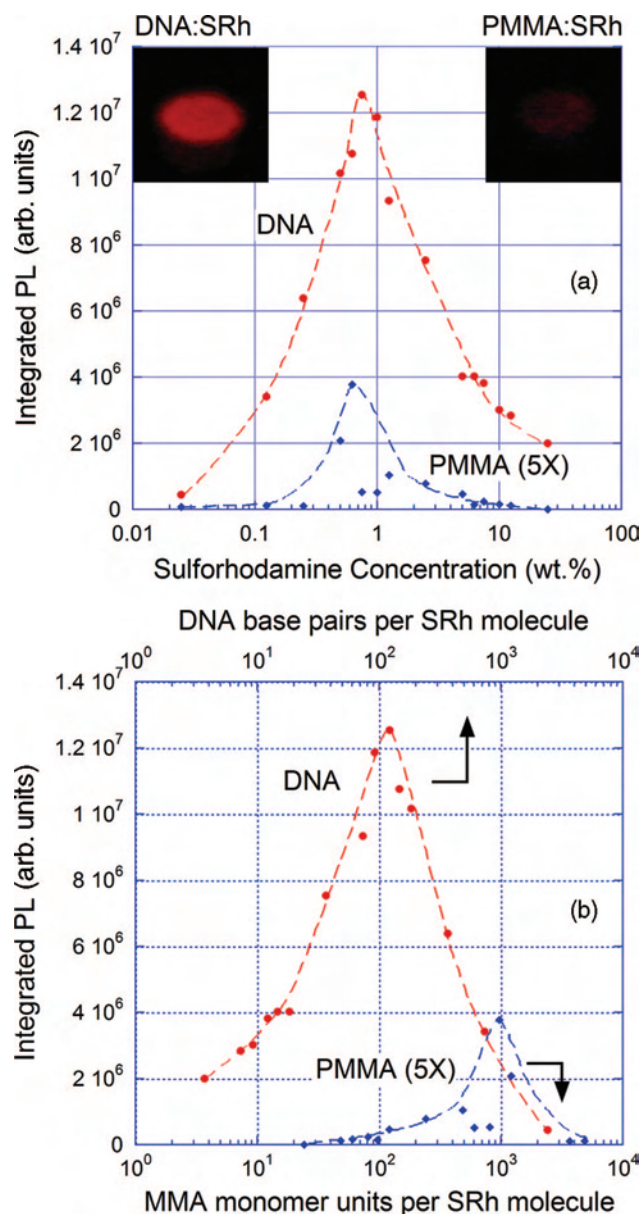


Fig. 4. (Color online) Integrated SRh photoluminescence versus concentration in DNA and PMMA. (a) SRh concentration by weight, (b) SRh molecules per DNA base pairs and PMMA monomer units. Inset, optical emission photographs for DNA and PMMA films doped with 0.7 wt. % SRh conc.

tion of these measurements is attributable to the fact that these DNA:SRh samples were in liquid form. Butanol solutions of DNA with different SRh concentrations were measured. Double stranded DNA has a characteristic CD peak at  $\sim 285$ – $287$  nm, as seen in the inset of Fig. 5. The intensity of the CD signal at this peak position is plotted in Fig. 5 as a function of the SRh doping concentration. From these measurements it is clear that the incorporated SRh molecules do not result in a net reduction in DNA chirality, even at concentrations as high as 25%. The maximum DNA CD signal occurs for an SRh concentration of  $\sim 5$  wt. %. It is tempting to interpret these results as evidence of highly efficient SRh intercalation into the

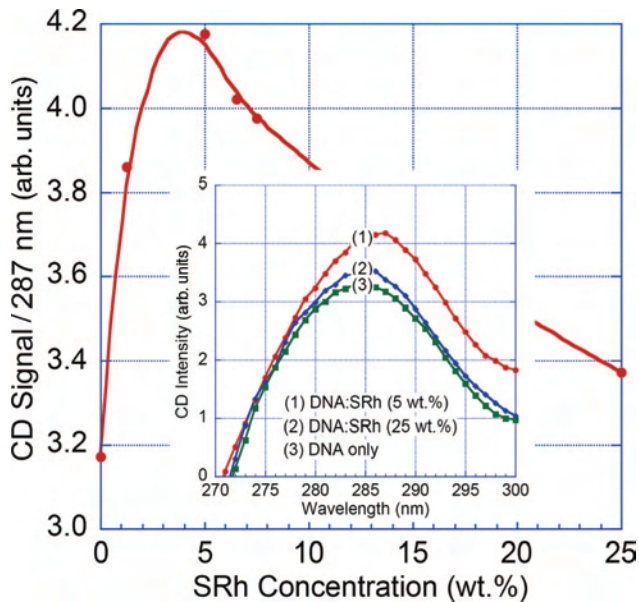


Fig. 5. (Color online) Circular dichroism intensity versus SRh concentration in DNA butanol solution. Inset, CD spectra for several DNA:SRh solutions.

DNA double helix (and associated efficient luminescence), since a concentration of 5 wt. % corresponds to one SRh molecule for every 20 base pairs. However, confirmation of this conclusion requires additional investigation. At this point, we can only confirm that either (major or minor) groove binding and/or intercalation has taken place.

#### B. Amplified Spontaneous Emission and Lasing

ASE and lasing in DNA:SRh were obtained by high-power optical pumping with the pulsed Nd:YAG laser at a wavelength of 532 nm. Figure 6 shows the basic features of the spectra obtained under ASE and las-

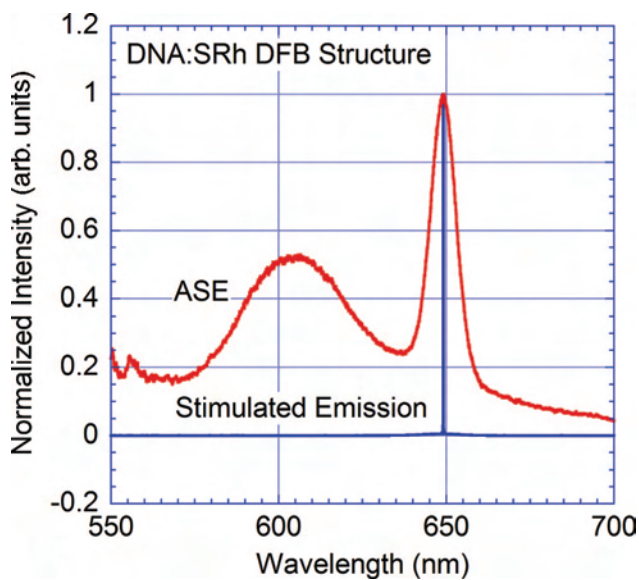


Fig. 6. (Color online) Amplified spontaneous and stimulated emission from DNA:SRh DFB structures.

ing pumping conditions. The ASE spectrum contains the peak at 605 nm observed in the PL spectrum obtained under low-power pumping with the He-Cd laser (see Fig. 2). The linewidth of the 605 nm peak is essentially the same in both cases:  $\sim 35$  nm. The ASE spectrum also contains a new peak at 650 nm, designated as the ASE peak of SRh. The  $\sim 10$  nm linewidth of this peak is much narrower than the PL peak at 605 nm. The intensity change and peak narrowing at 650 nm are typical features of an ASE process. Also included in Fig. 6 is a typical lasing spectrum from a DNA:SRh DFB structure. Under lasing pumping conditions, the PL emission peak at 605 nm is totally absent, and the emission peak width at 650 nm is less than 1 nm. Similar ASE and lasing spectral characteristics were observed for PMMA:SRh thin films and DFB structures.

The peak emission wavelength in SRh is known<sup>22</sup> to experience a redshift under ASE or lasing conditions. SRh in solution is reported<sup>23</sup> to have two lasing

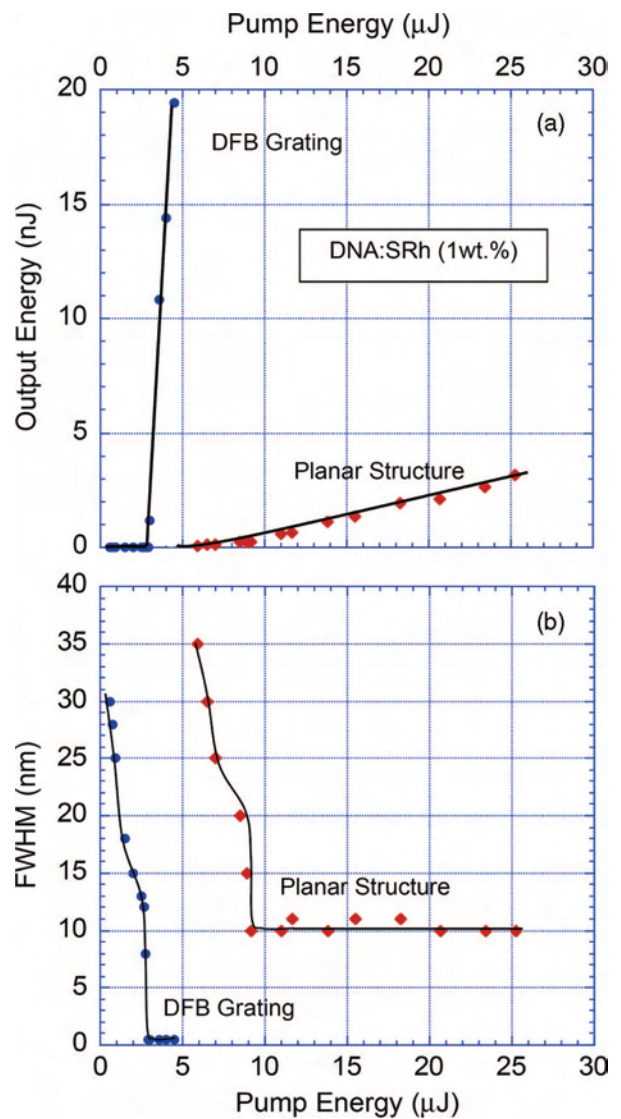


Fig. 7. (Color online) Output energy and linewidth from DNA:SRh DFB structures and thin film as a function of pump energy.

peaks at  $\sim 620$  and  $\sim 650$  nm. Since we have designed the feedback grating for 650 nm, the lasing occurs only at 650 nm.

The output energy and linewidth at 650 nm are shown in Figs. 7(a) and 7(b) as functions of pump energy for DNA:SRh (1 wt. %) DFB and planar structures. The output energy from the planar structure increases fairly gradually, with an increase in slope at  $\sim 9$   $\mu\text{J}$  pump energy. At the same pump energy, the emission linewidth experiences a sharp decrease with pump energy from the 35 nm FWHM typical of PL emission to the 10 nm linewidth typical of ASE. The ASE threshold of 9  $\mu\text{J}$  is equivalent to an energy density of  $\sim 95$   $\mu\text{J}/\text{cm}^2$ . For comparison, DNA films doped with rhodamine 6G (Rh6G)<sup>24</sup> and hemicyanine derivative<sup>25</sup> dyes have been reported with ASE thresholds of 2 and 0.5  $\text{mJ}/\text{cm}^2$ , respectively. The DFB grating output energy has an abrupt increase at 3  $\mu\text{J}$  pump energy, which is accompanied by a sharp drop in linewidth to  $\sim 0.4$  nm (instrument-limited

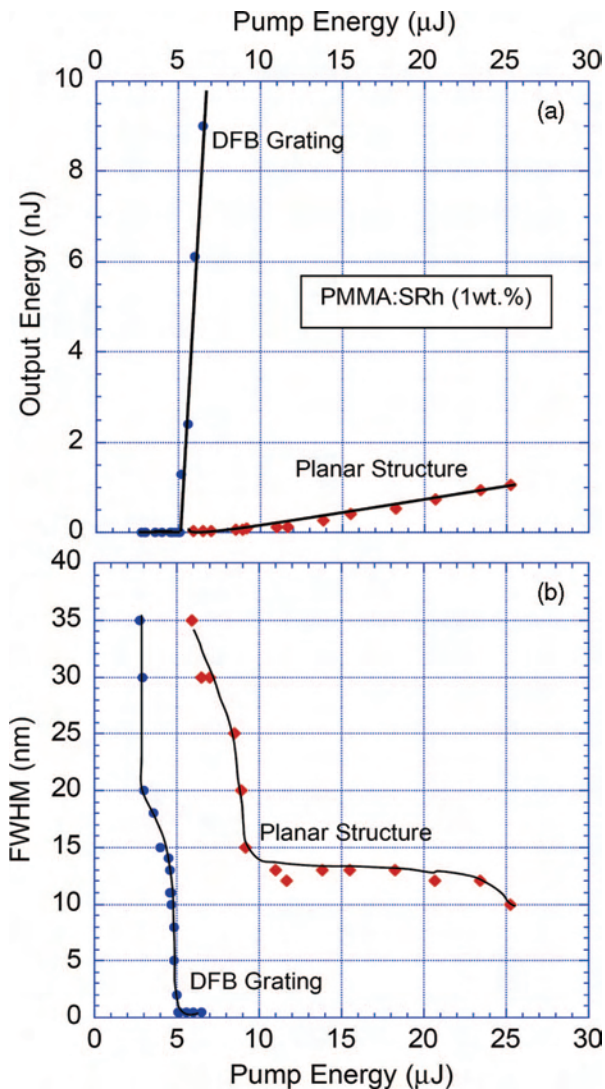


Fig. 8. (Color online) Output energy and linewidth from PMMA:SRh DFB structure and thin film as a function of pump energy.

resolution). This clearly identifies the lasing threshold for DNA:SRh at 3  $\mu\text{J}$ . This represents a pump energy density threshold of  $\sim 30$   $\mu\text{J}/\text{cm}^2$ , equivalent to a power density threshold of  $\sim 3.75$   $\text{kW}/\text{cm}^2$ . The energy density for lasing threshold is quite close to the 35  $\mu\text{J}/\text{cm}^2$  reported<sup>26</sup> for Rh6G dye in a small organic molecule host (Alq<sub>3</sub>). Lower threshold energies can be obtained by using dyes that have larger Stokes shifts, resulting in reduced self-absorption and hence increased optical gain in the waveguide.

The corresponding results for PMMA:SRh (1 wt. %) structures are shown in Fig. 8. In the case of the PMMA:SRh planar structure a similar change of slope occurs at  $\sim 11.5$   $\mu\text{J}$  accompanied by a drop in linewidth to  $\sim 12$ – $13$  nm. Lasing for the PMMA:SRh DFB grating occurs beyond a pump threshold of 5.1  $\mu\text{J}$ . This is equivalent to a pump energy density threshold of  $\sim 53$   $\mu\text{J}/\text{cm}^2$  and a power density threshold of  $\sim 6.63$   $\text{kW}/\text{cm}^2$ . The output energy in the lasing case is approximately an order of magnitude larger than the ASE case for both the DNA and the PMMA structures.

The output energy as a function of input energy for DNA:SRh (1 wt. %) and PMMA:SRh (1 wt. %) DFB gratings is shown in Fig. 9. The pump energy scale is of the order of a few microjoules, while the output lasing energy is on the order of tens of nanojoules above threshold. The slope efficiency ( $\eta$ ) is the efficiency of conversion of pump laser energy into output laser energy. The indicated slope efficiencies of 1.2% and 0.63% for the DNA and PMMA gratings, respectively, have been calculated based on the actual measured energy levels beyond their respective thresholds. However, one must bear in mind that not all of the pump energy is absorbed in the waveguide layer, and not all of the lasing emission is captured by the detector. The lasing, which occurs toward the

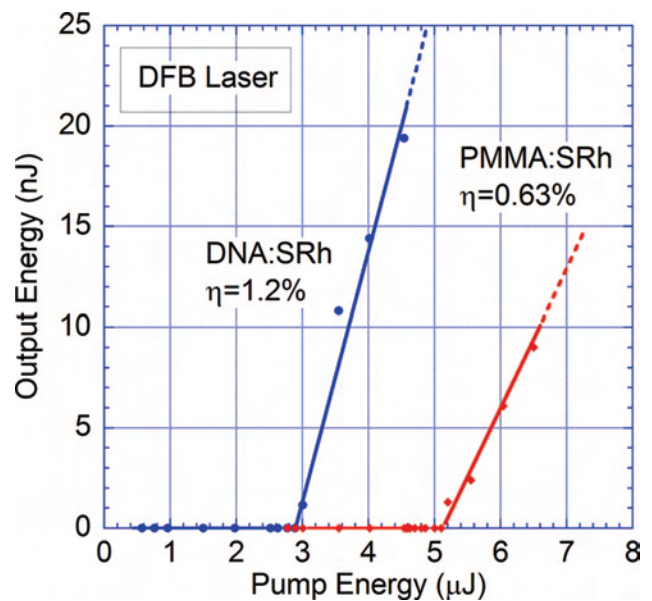


Fig. 9. (Color online) Input–output energy slope efficiency from DNA:SRh and PMMA:SRh DFB structures.

substrate, is absorbed by the Si wafer, and some of the lasing emission is waveguided in the DNA or the PMMA layer. Clearly, the DNA:SRh grating is more efficient than the PMMA:SRh grating, with a lower threshold energy and nearly twice the slope efficiency.

#### 4. Summary and Conclusions

Salmon DNA has been found to be an excellent polymer host for the laser dye sulforhodamine. The SRh doping concentration for maximum PL emission intensity was found to be equivalent to the ratio of DNA base pairs to dye molecules of 100:1. By comparison, SRh doped into the common polymer host PMMA exhibited much weaker PL and had an optimum concentration at a ratio of monomer (MMA) to SRh molecules of 1000:1. Lasing was obtained by fabricating second-order DFB gratings in both polymer hosts doped with SRh. The DNA:SRh grating had a threshold energy of 3  $\mu\text{J}$  versus 5.1  $\mu\text{J}$  for the PMMA:SRh grating and a slope efficiency nearly twice that, of the PMMA:SRh grating (1.2% versus 0.63%). While unambiguous proof of SRh intercalation in the DNA double helix has not yet been obtained, the addition of high concentration (up to 5 wt. %) of SRh molecules results in an increasing chirality of the DNA. Clearly, DNA is a promising material as a host for dye-based polymer lasers.

The authors express their appreciation to N. Ogata of Chitose Institute of Science and Technology, Chitose, Japan for providing the salmon DNA. The recent demonstration<sup>27</sup> of DNA thin films with nanometer thickness control by molecular beam deposition will greatly assist the fabrication of laser cavities with controllable and reproducible properties. The authors also thank E. Heckman of Anteon Corp. for assistance with the DNA sonication process and A. Altman of the University of Dayton for providing access to the Nd:YAG laser setup.

#### References

1. M. A. Stroschio and M. Dutta, "Integrated biological-semiconductor devices," *Proc. IEEE* **93**, 1772–1783 (2005).
2. A. J. Steckl, "DNA—a new material for photonics," *Nature Photon.* **1**, 3–5 (2007).
3. G. Zhang, L. Wang, and N. Ogata, "Optical and optoelectronic materials derived from biopolymer deoxyribonucleic acid (DNA)," in *Proc. SPIE* **4580**, 337–346 (2001).
4. J. G. Grote, E. M. Heckman, D. Diggs, J. A. Hagen, P. Yaney, A. J. Steckl, G. S. He, Q. Zheng, P. N. Prasad, J. Zetts, and F. K. Hopkins, "DNA-based materials for electro-optic applications," in *Proc. SPIE* **5934**, 593406-01 (2005).
5. J. Hagen, W. Li, A. J. Steckl, and J. G. Grote, "Enhanced emission efficiency in organic light-emitting diodes using deoxyribonucleic acid complex as an electron blocking layer," *Appl. Phys. Lett.* **88**, 171109 (2006).
6. Y. Oki, K. Ohno, and M. Maeda, "Tunable ultrashort pulse generation from a waveguided laser with premixed-dye-doped plastic film," *Jpn. J. Appl. Phys., Part 1* **37**, 6403–6407 (1998).
7. Y. Oki, T. Yoshiura, Y. Chisaki, and M. Maeda, "Fabrication of a distributed-feedback dye laser with a grating structure in its plastic waveguide," *Appl. Optics* **41**, 5030–5035 (2002).
8. K. D. Dorkenoo, O. Cregut, and A. Fort, "Organic plastic laser in holographic materials by photopolymerization," *Appl. Phys. Lett.* **84**, 2733–2735 (2004).
9. N. Tessler, "Lasers based on semiconducting organic materials," *Adv. Mater.* **11**, 363–370 (1999).
10. U. Scherf, S. Riechel, U. Lemmer, and R. F. Mahrt, "Conjugated polymers: lasing and stimulated emission," *Curr. Opin. Solid State Mater. Sci.* **5**, 143–154 (2001).
11. A. Costela, I. Garcia-Moreno, J. Barroso, and R. Sastre, "Laser performance of Coumarin 540A dye molecules in polymeric host media with different viscosities: from liquid solution to solid polymer matrix," *J. Appl. Phys.* **83**, 650–659 (1998).
12. N. Tsutsumi, T. Kawahira, and W. Sakai, "Amplified spontaneous emission and distributed feedback lasing from a conjugated compound in various polymer matrices," *Appl. Phys. Lett.* **83**, 2533–2535 (2003).
13. C. Metcalfe and J. A. Thomas, "Kinetically inert transition metal complexes that reversibly bind to DNA," *Chem. Soc. Rev.* **32**, 215–224 (2003).
14. L. Wang, J. Yoshida, and N. Ogata, "Self-assembled supramolecular films derived from marine deoxyribonucleic acid (DNA)-cationic surfactant complexes: large-scale preparation and optical and thermal properties," *Chem. Mater.* **13**, 1273–1281 (2001).
15. K. Tanaka and Y. Okahata, "A DNA-lipid complex in organic media and formation of an aligned cast film," *J. Am. Chem. Soc.* **118**, 10679–10683 (1996).
16. E. Heckman, J. Hagen, P. Yaney, J. Grote, and F. K. Hopkins, "Processing techniques for deoxyribonucleic acid: biopolymer for photonics applications," *Appl. Phys. Lett.* **87**, 211115 (2005).
17. E. T. Knobbe, B. Dunn, P. D. Fuqua, and F. Nishida, "Laser behavior and photostability characteristics of organic dye doped silicate gel materials," *Appl. Opt.* **29**, 2729–2733 (1990).
18. M. D. Rahn and T. A. King, "Comparison of laser performance of dye molecules in sol-gel, polycom, ormosil, and poly(methyl methacrylate) host media," *Appl. Opt.* **34**, 8260–8271 (1995).
19. H. Kogelnik and C. V. Shank, "Stimulated emission in a periodic structure," *Appl. Phys. Lett.* **18**, 152–154 (1971).
20. H. Junicke, J. R. Hart, J. Kisko, O. Glebov, I. R. Kirsch, and J. K. Barton, "A rhodium(III) complex for high-affinity DNA base-pair mismatch recognition," *Proc. Natl. Acad. Sci. USA* **100**, 3737–3742 (2003).
21. A. Rodger and B. Norden, *Circular Dichroism and Linear Dichroism* (Oxford U. Press, 1997).
22. N. M. Lawandi, R. M. Balachandran, A. S. L. Gomes, and E. Sauvain, "Laser action in strongly scattering media," *Nature* **368**, 436–438 (1994).
23. W. L. Sha, C.-H. Liu, F. Liu, and R. R. Alfano, "Competition between two lasing modes of sulforhodamine 640 in highly scattering media," *Opt. Lett.* **21**, 1277–1279 (1996).
24. Y. Kawabe, L. Wang, S. Horinouchi, and N. Ogata, "Amplified spontaneous emission from fluorescent-dye-doped DNA-surfactant complex films," *Adv. Mater.* **12**, 1281–1283 (2000).
25. Y. Kawabe, L. Wang, T. Nakamura, and N. Ogata, "Thin-film lasers based on dye-deoxyribonucleic acid-lipid complexes," *Appl. Phys. Lett.* **81**, 1372–1374 (2002).
26. V. G. Kozlov, V. Bulovic, P. E. Burrows, M. Baldo, V. B. Khalfin, G. Partharathy, and S. R. Forrest, "Study of lasing action based on Förster energy transfer in optically pumped organic semiconductor thin films," *J. Appl. Phys.* **84**, 4096–4108 (1998).
27. J. A. Hagen, W. X. Li, H. Spaeth, J. G. Grote, and A. J. Steckl, "Molecular beam deposition of DNA nanometer films," *Nano Lett.* **7**, 133–137 (2007).